

# Plasma rotation effects on neoclassical tearing modes

D. Chandra, A. Sen and P. K. Kaw

*Institute for Plasma Research, Bhat, Gandhinagar - 382428, India*

(Received: 20 November 2009 / Accepted: 6 May 2010)

The effect of an equilibrium sheared flow on the nonlinear evolution of a neoclassical tearing mode is investigated by estimating the influence it has on the inner and outer layer dynamics of the mode. Two complementary approaches are adopted. A generalized Rutherford model calculation is carried out to estimate the flow contributions to the polarization current term in the inner layer. For the outer layer, flow induced changes in the stability parameter  $\Delta'$  are estimated with the help of a 3D initial value reduced MHD code (NEAR). For realistic parameters it is found that the outer layer modification is the dominant one and the scaling of  $\Delta'$  with the flow shear parameter appears to agree with recent experimental observations.

Keywords: sheared flow, neoclassical tearing mode, Rutherford model, stability parameter

## 1. Introduction

The influence of plasma rotation and rotation shear on the excitation and stability of various MHD modes has been an important topic of investigation in tokamak research for a number of years now [1–12]. In particular their effect on tearing modes has attracted a great deal of past theoretical work and has led to the identification of many basic results. More recently the attention has shifted to neoclassical tearing modes (NTMs) which pose a potential threat to achievement of high  $\beta$  in present day long pulsed tokamak experiments and in future operational scenarios of ITER [13–15]. With the availability of better diagnostics and means for controlling the direction and amount of plasma flow, several recent tokamak experiments have addressed the issue of establishing the nature of correlation between the amount of flow (and flow shear) and the threshold  $\beta$  for the onset of an NTM as well as the size of the saturated magnetic island. The experimental data show a clear evidence of flow (and flow shear) induced modification of both the onset threshold  $\beta_N$  and the saturation size of the island. On DIII-D experiments [16], through controlled variation of co and counter NBI beams, it has been found that, in general, decreasing toroidal plasma flow impairs NTM (tearing mode) stability. With decreased flow, existing 3/2 islands can become larger and stable 2/1 modes can get excited. Thus with lower rotation the NTM onset has a stronger drive (lower  $\beta_N$ ). Although in most cases it is difficult to experimentally separate the flow effects from flow shear effects, on many shots where it has been possible to obtain a good measure of the flow profile it is observed that flow shear has a strong influence on the mode stability. By increasing the amount of flow shear it is possible to reduce the size of an existing 3/2 magnetic island. Such observations have been made for a variety of operational scenarios (H mode plasmas, sawteething plasmas as well as reversed shear plasmas) and on multiple machines (JET, AUG, NSTX etc.) [14, 16]. There is also strong evidence (though not entirely unambiguous) that the sign

of the flow shear matters and hence a tailoring of the flow profile can be an important factor in the control or suppression of NTMs. Theoretical understanding of these experimental observations is still very limited. While it is known from past model studies that flows and flow shear can bring about profound changes in the mode dynamics near the resonant layer (inner layer) as well as in the stability index  $\Delta'$  (outer layer effect), a quantitative estimate of these effects is not available to date. On the basis of heuristic arguments, experimental observations of the DIII-D machine have been interpreted in terms of a change in the stability index  $\Delta'$  and an empirical linear scaling of the stability index with the flow shear has been projected [16]. Comparison of multi-machine data to arrive at a better understanding and identification of the underlying physical effects is currently being carried out by various groups and is also a high priority study topic for ITER.

Our present work is motivated by a desire to provide some theoretical understanding of the observed flow effects through a combination of analytical and numerical modeling. To gain some insight into the flow induced modifications of the inner layer dynamics we have carried out a model two fluid calculation and derived a generalized Rutherford equation which incorporates flow contributions to the polarization current term. To study the influence on  $\Delta'$  we have used a 3D initial value reduced MHD code (NEAR) and investigated the evolution of a single helicity NTM for various flow profiles and estimated the changes in the stability index from measurements of the saturated island width. From a numerical comparison of the inner and outer layer modifications, for a set of realistic parameters, we find that the dominant contribution to the NTM growth rate and saturation width arises from the  $\Delta'$  modification rather than the inner layer effects. The numerical simulations also display a near linear scaling of  $\Delta'$  with the amount of flow shear - a result that is in qualitative agreement with the observed experimental results on DIII-D.

author's e-mail: [abhijit@ipr.res.in](mailto:abhijit@ipr.res.in)

Our paper is organized as follows. In the next section we present our analytical calculations for the flow effects on the inner layer dynamics. Section 3 is devoted to an estimation of changes in  $\Delta'$  through numerical simulations on the code NEAR. In the final section we discuss and compare the results of sections 2 and 3 and make some concluding remarks.

## 2. Flow effects on the Inner Layer dynamics

We consider a single helicity magnetic perturbation moving across an equilibrium magnetic field. In the vicinity of a resonant surface where the helicity of the perturbation matches the pitch of the equilibrium field (i.e.  $q(r_s) = m/n$ ,  $q$  is the safety factor), the magnetic field can be expressed in terms of an effective flux function  $\psi$ ,

$$\psi = -\frac{B_0}{L_s} \frac{x^2}{2} + \tilde{\psi} \cos \xi \quad (1)$$

Here  $B_0$  is the average equilibrium toroidal magnetic field,  $x = r - r_s$  is the distance from the rational surface,  $L_s = qR/s$  is the shear length,  $s = r_s q'/q$  and  $\xi = m\hat{\theta} - \int \omega(t') dt'$  where  $\hat{\theta} = \theta - \zeta/q_s$  is the helical coordinate with  $\theta$  denoting the poloidal angle and  $\zeta$  the toroidal angle. Note that for  $m \geq 2$ , when the constant  $\tilde{\psi}$  approximation holds, the magnetic island halfwidth is given by,

$$W = \left( \frac{4L_s \tilde{\psi}}{B_0} \right)^{1/2} \quad (2)$$

The nonlinear evolution equation of the magnetic island is derived from the matching conditions obtained by integrating Ampere's equation across the nonlinear region.

$$\int_{-\pi}^{\pi} d\xi \cos \xi \int_{-\infty}^{\infty} dx J_{\parallel} = \frac{c}{4\pi} \Delta'_c \pi \tilde{\psi} \quad (3)$$

$$\int_{-\pi}^{\pi} d\xi \sin \xi \int_{-\infty}^{\infty} dx J_{\parallel} = \frac{c}{4\pi} \Delta'_s \pi \tilde{\psi} \quad (4)$$

where the matching parameters  $\Delta'_{c,s}$  are determined from the outer (linear) region and are assumed to be given by ideal MHD equations. The longitudinal current needs to be obtained from the parallel Ohm's law,

$$J_{\parallel} = \sigma_{neo} \left( -\nabla_{\parallel} \Phi + \frac{1}{c} \frac{\partial}{\partial t} \psi(t) \right) - \frac{\mu_e}{v_{ei}} \frac{c}{B_{\theta}} \frac{dp}{dx} \quad (5)$$

where  $\mu_e$  is the viscosity coefficient,  $v_{ei}$  is the electron collision frequency,  $B_{\theta}$  is the poloidal magnetic field,  $p$  is the plasma pressure and  $\sigma_{neo}$  is the neoclassical conductivity. The last term on the RHS is the perturbed bootstrap current which is responsible for driving the neoclassical tearing modes. For the low frequency tearing mode, quasineutrality condition holds so that we have,

$$\nabla_{\parallel} J_{\parallel} + \nabla_{\perp} \cdot \mathbf{J}_{\perp} = 0 \quad (6)$$

where the perpendicular component of the total current is proportional to the plasma inertia through the ion polarization drift. With the substitution for  $\mathbf{J}_{\perp}$ , (6) takes the form,

$$\nabla_{\parallel} J_{\parallel} - \frac{c^2}{4\pi v_A^2} \frac{d_0}{dt} \nabla_{\perp}^2 \left( \Phi + \frac{p_i}{en} \right) = 0 \quad (7)$$

where the operator  $d_0/dt$  can be written as,

$$\begin{aligned} \frac{d_0}{dt} &\equiv \frac{\partial}{\partial t} + (\mathbf{v}_E + \mathbf{v}_{\parallel 0}) \cdot \nabla \\ &= -\psi_s \left\{ (\omega - \omega_{*pi}) x - \frac{k_{\theta} c}{B_0} \Phi, \right\} \\ &\quad + \frac{k_{\theta} \psi_x v_{\parallel 0}}{B_0} \frac{\partial}{\partial \xi} \end{aligned} \quad (8)$$

Here Poisson bracket  $\{\alpha, \beta\} = \frac{\partial \alpha}{\partial \psi} \frac{\partial \beta}{\partial \xi} - \frac{\partial \alpha}{\partial \xi} \frac{\partial \beta}{\partial \psi}$ ,  $\omega_{*pi}$  is the ion diamagnetic frequency,  $\omega_{*pi} = k_{\theta} c T_i p'_{0i} / (e B p_{0i})$  [17, 18],  $\mathbf{v}_E$  is the  $\mathbf{E} \times \mathbf{B}$  drift component and  $\mathbf{v}_{\parallel 0}$  is the parallel component of the equilibrium sheared flow.

To solve (7) we need to get an expression for  $\Phi$ , the electrostatic potential. Note that to the lowest order in Ohm's law,  $E_{\parallel} = \nabla_{\parallel} \Phi + \frac{1}{c} \frac{\partial}{\partial t} \psi(t) \approx 0$ , which implies a near cancellation of the electrostatic field by the inductive electric field. By transforming the coordinates from  $(x, y) \rightarrow (\psi, \xi)$  we can write  $\nabla_{\parallel}$  as,

$$\nabla_{\parallel} = \frac{k_{\theta}}{B_0} \frac{\partial \psi}{\partial x} \left( \frac{\partial}{\partial \xi} \right)_{\psi} \quad (9)$$

where  $k_{\theta} = m/r_s$  is the poloidal wave vector and derivative with respect to  $\xi$  is to be evaluated at constant  $\psi$ .

Using the above expression for  $\nabla_{\parallel}$  and integrating  $E_{\parallel} \approx 0$ , in  $\xi$  we get,

$$\Phi = \frac{B_0 \omega x}{ck_{\theta}} + f(\psi) \quad (10)$$

where  $f(\psi)$  the integration constant is an arbitrary function of  $\psi$ , and needs to be determined from the boundary conditions. In carrying out the integration one also uses the identity,

$$\frac{\tilde{\psi} \sin \xi}{\psi_x} = \left( \frac{\partial x}{\partial \xi} \right)_{\psi} \quad (11)$$

To account for the flow shear we write  $\Phi$  and  $v_{\parallel 0}$  as,

$$\Phi = \Phi'_0 x + \Phi''_0 \frac{x^2}{2} + \tilde{\phi}(x, \xi) \quad (12)$$

$$v_{\parallel 0} = v_{\parallel s} + v'_{\parallel s} x \quad (13)$$

Equating both the expressions for  $\Phi$  (i.e. using expressions (10) and (12)) we can write,

$$\tilde{\phi} = \frac{B_0}{ck_{\theta}} (\omega - \omega_E) x - \frac{B_0}{ck_{\theta}} \frac{\omega'_E}{2} x^2 + f(\psi) \quad (14)$$

where  $\omega_E = k_{\theta} c \Phi'_0 / B_0$  is the drift frequency due to the radial equilibrium electric field created by the magnetic perturbation moving across  $B_0$  and  $\tilde{\phi}$  is the perturbed  $\Phi$ . An

appropriate choice of  $f(\psi)$  such that  $\tilde{\phi}$  vanishes for large  $x$  (i.e. far away from the island) is,

$$f(\psi) = -\frac{B_0}{ck_\theta}(\omega - \omega_E)\lambda(\psi) - \frac{B_0}{ck_\theta} \frac{\omega'_E}{2} \lambda^2(\psi) \quad (15)$$

Substituting for  $f(\psi)$  we get,

$$\tilde{\phi} = \frac{B_0}{ck_\theta}(\omega - \omega_E)(x - \lambda) - \frac{B_0}{ck_\theta} \frac{\omega'_E}{2} (x^2 - \lambda^2) \quad (16)$$

Here the function  $\lambda(\psi)$  is chosen to be zero inside the magnetic separatrix and  $\lambda(\psi) \rightarrow x$  in the region  $x \gg W$  [17, 18]. We have taken the following form of  $\lambda(\psi)$  in the outer region,

$$\lambda(\psi) = \frac{W}{\sqrt{2}} \left[ \left( -\frac{\psi}{\tilde{\psi}} \right)^{1/2} - 1 \right] \quad (17)$$

where  $W$  is the magnetic island half width as defined in (2).

Following standard procedure we now integrate Eq. (7) using Eqs. (12), (13) and (16) to obtain the parallel component of current as,

$$\begin{aligned} J_{\parallel} &= A(\psi)(\cos \xi - \langle \cos \xi \rangle) \\ &+ B(\psi)(x^3 - \langle x^3 \rangle) + \frac{\sigma_{\parallel}}{c} \frac{\partial \tilde{\psi}}{\partial t} \langle \cos \xi \rangle \\ &- \frac{\mu_e c}{v_{ei} B_\theta} \left\langle \frac{\partial \psi}{\partial x} \frac{\partial p}{\partial \psi} \right\rangle \end{aligned} \quad (18)$$

where,

$$\begin{aligned} A(\psi) &= \frac{cB_0^4 W^2}{8\pi v_A^2 k_\theta^2 L_s^2} \left[ \frac{\omega'_E}{2} \frac{\partial \lambda^2}{\partial \psi} - (\omega - \omega_E) \frac{\partial \lambda}{\partial \psi} \right. \\ &\left. + \frac{k_\theta v_{\parallel s}}{B_0} \right] \left[ \frac{\omega'_E}{2} \frac{\partial^2 \lambda^2}{\partial \psi^2} - (\omega - \omega_E - \omega_{*pi}) \frac{\partial^2 \lambda}{\partial \psi^2} \right] \end{aligned} \quad (19)$$

$$\begin{aligned} B(\psi) &= \frac{cB_0^4}{4\pi v_A^2 k_\theta^2 L_s^2} \frac{k_\theta v'_{\parallel s}}{B_0} \left[ \frac{\omega'_E}{2} \frac{\partial^2 \lambda^2}{\partial \psi^2} \right. \\ &\left. - (\omega - \omega_E - \omega_{*pi}) \frac{\partial^2 \lambda}{\partial \psi^2} \right] \end{aligned} \quad (20)$$

and the flux surface average operator  $\langle \dots \rangle$  is defined as,

$$\langle \dots \rangle = \oint \frac{\frac{(\dots)}{\frac{\partial \psi}{\partial x}} d\xi}{\frac{1}{\frac{\partial \psi}{\partial x}} d\xi} \quad (21)$$

We now use Eq. (18) in the matching condition (3), to arrive at the following island evolution equation,

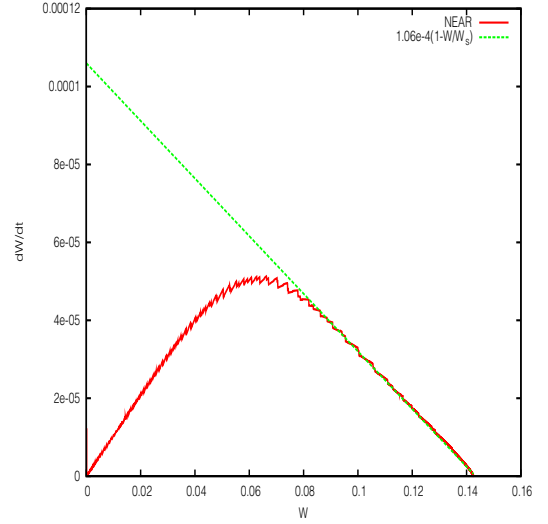


Fig. 1 Rate of change of island width vs island width

$$\begin{aligned} G_1 \frac{\partial W}{\partial t} &= D_R^{neo} \left[ \frac{\Delta'_c}{4} + G_2 \frac{\sqrt{\epsilon} \beta_\theta \frac{L_q}{L_p}}{W} \frac{W^2}{W^2 + W_\chi^2} \right. \\ &- G_3 \frac{D_I}{\sqrt{W^2 + 0.65W_\chi^2}} + G_4 \frac{L_s^2}{k_\theta^2 v_A^2} \frac{(\omega - \omega_E)(\omega - \omega_E - \omega_*)}{W^3} \\ &+ G_5 \frac{L_s^2}{k_\theta^2 v_A^2} \frac{\omega'_E{}^2}{W} - G_6 \frac{L_s}{k_\theta v_A} \frac{v_{\parallel s}}{v_A} \frac{\omega'_E}{W} \\ &\left. - G_7 \frac{L_s}{k_\theta v_A} \frac{v'_{\parallel s}}{v_A} \frac{(\omega - \omega_E - \omega_*)}{W} - G_8 \frac{c_s^2}{v_A^2} \frac{1}{W} \right] \end{aligned} \quad (22)$$

where,  $D_R^{neo} = c^2/4\pi\sigma_{neo}$  is the magnetic diffusion coefficient calculated using the neoclassical resistivity,  $\beta_\theta = 8\pi p_e/B_\theta^2$ ,  $L_p = -(d \ln p/dr)^{-1}$ ,  $L_q = (d \ln q/dr)^{-1}$ ,  $L_s = qR/s$ ,  $D_I = -2(q^2 - 1)rp'/(s^2 B_0^2)$  is the resistive interchange parameter,  $s = rq'/q$  is the magnetic shear and  $v_{\parallel 0}$  is the average parallel flow velocity. The coefficients  $G_1$  to  $G_6$  are defined in the Appendix and their numerical values are:  $G_1 = 0.41, G_2 = 0.58, G_3 = 6.35, G_4 = 5.7, G_5 = 0.24, G_6 = 0.77, G_7 = 2.05$  and  $G_8 = 1.9$ . For evaluating the neoclassical contribution we have adopted the standard procedure outlined in [18] where  $\mu_e \simeq \sqrt{\epsilon} v_{ei}$  for the long mean-free-path regime has been used and  $\omega_* = \omega_{*pi} + k\omega_{*T}$  [18], with  $\omega_{*T} = k_\theta c T'_i / e B_0$ . The factor  $W^2/(W^2 + W_\chi^2)$  in the neoclassical term is the usual effect associated with finite radial thermal diffusion and sets a critical island width  $W_\chi = \sqrt{\frac{RqL_q}{m}} \left( \frac{\chi_\perp}{\chi_\parallel} \right)^{1/4}$ , below which radial transport becomes significant and the pressure is no longer flattened across the island. In the above expression for the island width evolution equation (22), the term proportional to the  $\omega'_E{}^2$  arises purely from the perpendicular flow shear contributions and the term proportional to  $v_{\parallel s} \omega'_E$  is due to the combination of parallel flow and perpendicular flow shear.

In eqn. (22), the term proportional to  $G_2$  is the usual

NTM driving term arising from the perturbed bootstrap current and the term with the coefficient  $G_3$  is the Glasser-Green-Johnson (GGJ) contribution representing a stabilization effect due to the toroidal curvature. The next term involving  $G_4$  is a flow term which is destabilizing in nature except for the window  $0 < \omega - \omega_E < \omega_{*pi}$  and has been discussed in several past works [18–21]. The term involving  $G_5$  arises purely due to perpendicular flow shear on tearing modes and from the sign in front of it, is always destabilizing in nature. The next two terms proportional to  $G_6$  and  $G_7$  depend upon parallel shear flow. These terms are proportional to both flow shear as well as the flow velocity at the resonant surface and can change sign depending on the signs of the flow shear and flow. These last two terms also differ in other ways from the  $G_4$  term. The  $G_4$  term goes as  $\frac{1}{W^3}$ . So for NTMs which begin with a finite threshold island size, the effect of this term diminishes as the island evolves as its magnitude decreases more rapidly than the driving NTM term. The numerator of the term also remains small because island rotation frequency  $\omega$  is usually close to the flow frequency  $\omega_E$  i.e.  $(\omega - \omega_E)$  is small. But the shear terms go as  $\frac{1}{W}$  which are similar to the way the NTM driving term varies. So their effects remain similar throughout the evolution of NTM and can influence the full NTM dynamics from threshold to saturation. Secondly, the  $G_4$  term depends mainly on the flow frequency whereas the new terms depend also on the flow gradient. We should also mention here that the terms parallel and perpendicular flows in the context of a toroidal flow velocity in a tokamak, refer to the parallel and perpendicular (to the magnetic field) projections of the flow velocity and are therefore finite quantities. In other words for a purely toroidal flow (with zero poloidal velocity) there is still a perpendicular component of the flow because the magnetic field lines are not purely toroidal. We defer the numerical estimates of these flow induced contributions to the inner layer to the final section when we carry out a comparison with the changes in the outer layer dynamics.

### 3. Flow effects on the Outer Layer dynamics

As discussed in past model calculations, equilibrium flows can also affect the stability index of a tearing mode by modifying the shape of the eigenfunction of the outer layer MHD equations. One way of estimating this influence is to set up an appropriate modified Newcomb equation which incorporates the inertial contribution of flow and solve this equation for various flow profiles. Such a calculation was done for a cylindrical model in [7, 22] and earlier in the slab approximation [5]. However for a toroidal configuration such a formulation is quite difficult and we have instead chosen to address this issue through direct numerical simulations using a fully toroidal reduced MHD code called NEAR. This code solves a set of gen-

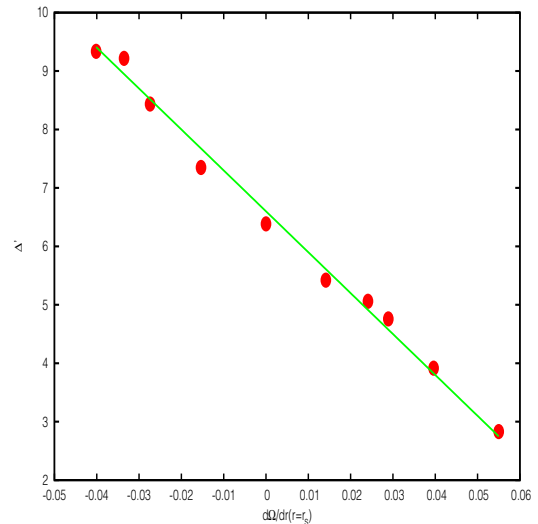


Fig. 2 Stability index  $\Delta'$  vs flow shear.

eralized reduced MHD equations that are valid for arbitrary aspect ratios and can correctly handle sub-Alfvénic toroidal equilibrium flows. Details of the equations and the code have been extensively discussed in the past and can be found in [13, 23]. The code has been well benchmarked for both linear and nonlinear classical tearing modes as well as NTMs and has also been employed previously to study the nonlinear evolution of NTMs in the presence of toroidal sheared flows [13]. These studies have shown that sheared toroidal flows can significantly alter the stability and saturation properties of single helicity NTMs. Our objective in the present work is to extract the information about the corresponding changes in the stability index  $\Delta'$  as a function of the flow characteristics. To accomplish this we have examined the temporal evolution of the mode upto its saturation. In Fig. 1 we have plotted the rate of change of the island width as a function of the island width. Earlier analytical studies [24] have shown that close to saturation the island evolution equation for a tearing mode can be represented by a simple equation of the form,

$$\frac{dW}{dt} = \frac{1.66\Delta'}{S} \left[ 1 - \frac{W}{W_s} \right] \quad (23)$$

As is clear from Fig. 1 the island evolution rate indeed satisfies such a model form close to saturation and the slope of the linear curve then directly gives us  $\frac{1.66\Delta'}{S}$  and hence  $\Delta'$ . We have evaluated  $\Delta'$  with and without equilibrium flow and thereby estimated the changes brought about by flow. In Fig. 2 we have plotted the values of  $\Delta'$  as a function of the amount of flow shear and Fig. 3 provides a variation of the saturated island width with flow shear. Both figures clearly show that increase of positive flow shear has a stabilizing effect on the stability index as well as on the saturated island width. Interestingly the scaling of  $\Delta'$  with flow shear shows a linear dependence - a trend that is in qualitative agreement with the empirical scaling seen in the experimental data of DIII-D. However a detailed quantita-

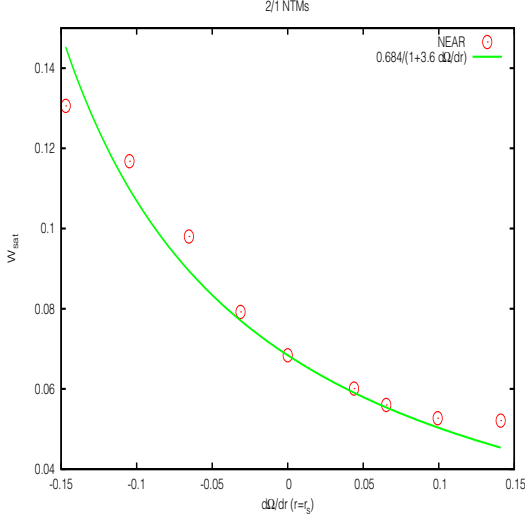


Fig. 3 Saturated island width vs flow shear

tive comparison with the experimental results is beyond the scope and ability of the model calculations presented here. In the next section we will however carry out a comparison of the flow induced effects in the inner and outer layer dynamics to get some quantitative idea of their relative importance.

#### 4. Discussion and Conclusion

As demonstrated in Secs. 2 and 3, sheared flow can influence the dynamics of a tearing mode or an NTM in two different ways. It can affect the dynamics near the mode resonant surface (the inner layer) by its contributions to the polarization current term and it can alter the stability index  $\Delta'$  by influencing the outer layer MHD mode structure. We now carry out an approximate quantitative estimate of these two effects to assess their relative importance. As a common physical parameter space we choose the typical values we have used for our numerical simulations on NEAR, namely,  $r_s/a=0.565$ ,  $\beta_0=0.002$ ,  $R/R_0=1.001$ ,  $q_s=2.0$ ,  $s=0.743$ ,  $\Omega_s \tau_A = 3.53 \times 10^{-3}$ ,  $d(\Omega_s \tau_A)/d(r/a) = 6.34 \times 10^{-2}$  and  $W_s/a=0.103$ . For such a case we have  $\Delta'a=2.108$  while in the absence of flow we get  $\Delta'a=6.385$  - a change of about 4.2. For these same parameters, the contributions from the flow shear terms which are related to  $G_5$ ,  $G_6$  and  $G_7$  coefficients are approximately,  $\frac{5.6 \times 10^{-4}}{(W/a)}$ ,  $\frac{1.3 \times 10^{-4}}{(W/a)}$  and  $\frac{3.5 \times 10^{-4}}{(W/a)}$  respectively. So even for  $W/a = 0.01$  at the beginning of the Rutherford phase the contributions from these terms remain of the order of  $10^{-2}$  and are quite small compared to the corresponding change in  $\Delta'$ . Thus from our model calculations it appears that the outer layer modifications are more pronounced compared to the inner layer ones in the parametric space that we have examined. It should be mentioned here that although the toroidal flow velocity in our numerical code is sub-Alfvénic its perpendicular (to the magnetic field) component is comparable to the poloidal Alfvén velocity - the latter being low for our

choice of parameter values. This makes it possible for the flow to influence the outer layer dynamics.

To conclude, our analytic calculations based on the generalized Rutherford model and the numerical simulations on NEAR provide separate estimates of the effect of shear flow on the inner and outer layer dynamics of a neoclassical tearing mode. Approximate numerical estimates of the two contributions show that the outer layer modifications are more significant. The results from NEAR further show that positive flow shear has a stabilizing influence and the stability index follows a linear scaling with the amount of flow shear. These results are in qualitative agreement with recent experimental findings [14, 16]. These preliminary and qualitative results which provide useful and encouraging insights into present experimental observations will we hope lead to more detailed investigations on improved models coupled to state-of-the-art codes like NIMROD for a better quantitative extrapolation of these effects to ITER.

#### Appendix: Calculation of the numerical coefficients in the island evolution equation

The G coefficients in the equation (22) have been evaluated numerically. Here  $G_1$  is given by the integral,

$$G_1 = \frac{1}{2\sqrt{2}\pi} \int_{-1}^{\infty} d\alpha \langle \cos \xi \rangle^2 \int_{-\pi}^{\pi} \frac{d\xi}{(\cos \xi + \alpha)^{1/2}} \quad (24)$$

where,  $\alpha = -(\psi/\tilde{\psi})$ . Now by putting  $\alpha = 2k^2 - 1$  we have got,

$$G_1 = \frac{4}{\pi} \int_0^1 k dk \langle \cos \xi \rangle_{in}^2 K(k^2) + \frac{4}{\pi} \int_1^{\infty} dk \langle \cos \xi \rangle_{out}^2 K\left(\frac{1}{k^2}\right)$$

where,

$$\langle \cos \xi \rangle_{in} = 2 \frac{E(k^2)}{K(k^2)} - 1, k < 1$$

$$\langle \cos \xi \rangle_{out} = 1 + 2k^2 \left[ \frac{E\left(\frac{1}{k^2}\right)}{K\left(\frac{1}{k^2}\right)} - 1 \right], k > 1$$

and E, K are the elliptic integrals of first and second kind respectively. Here, the inner region of the island is correspond to  $k < 1$  where the magnetic field lines are closed and the outer region is correspond to  $k > 1$  with an open magnetic field lines.

Similarly other coefficients are given by,

$$\begin{aligned} G_4 &= -\frac{8\sqrt{2}}{\pi} \int_{-1}^{\infty} d\alpha (\langle \cos^2 \xi \rangle - \langle \cos \xi \rangle^2) \frac{\partial g}{\partial \alpha} \frac{\partial^2 g}{\partial \alpha^2} \\ &\quad \times \int_{-\pi}^{\pi} \frac{d\xi}{(\cos \xi + \alpha)^{1/2}} \\ &= -\frac{8}{\pi} \int_0^{\infty} \frac{dk}{k^2} (\langle \cos^2 \xi \rangle_{out} - \langle \cos \xi \rangle_{out}^2) \\ &\quad \times \frac{\partial g}{\partial k} \frac{\partial}{\partial k} \left( \frac{1}{4k} \frac{\partial g}{\partial k} \right) K\left(\frac{1}{k^2}\right) \quad (25) \end{aligned}$$

$$\begin{aligned}
G_5 &= \frac{\sqrt{2}}{\pi} \int_{-1}^{\infty} d\alpha (\langle \cos^2 \xi \rangle - \langle \cos \xi \rangle^2) \frac{\partial g^2}{\partial \alpha} \frac{\partial^2 g^2}{\partial \alpha^2} \\
&\quad \times \int_{-\pi}^{\pi} \frac{d\xi}{(\cos \xi + \alpha)^{1/2}} \\
&= \frac{1}{\pi} \int_1^{\infty} \frac{dk}{k^2} (\langle \cos^2 \xi \rangle_{out} - \langle \cos \xi \rangle_{out}^2) \\
&\quad \times \frac{\partial g^2}{\partial k} \frac{\partial}{\partial k} \left( \frac{1}{4k} \frac{\partial g^2}{\partial k} \right) K\left(\frac{1}{k^2}\right)
\end{aligned} \tag{26}$$

$$\begin{aligned}
G_6 &= \frac{\sqrt{2}}{\pi} \int_{-1}^{\infty} d\alpha (\langle \cos^2 \xi \rangle - \langle \cos \xi \rangle^2) \frac{\partial^2 g^2}{\partial \alpha^2} \\
&\quad \times \int_{-\pi}^{\pi} \frac{d\xi}{(\cos \xi + \alpha)^{1/2}} \\
&= \frac{4}{\pi} \int_1^{\infty} \frac{dk}{k} (\langle \cos^2 \xi \rangle_{out} - \langle \cos \xi \rangle_{out}^2) \\
&\quad \times \frac{\partial}{\partial k} \left( \frac{1}{4k} \frac{\partial g^2}{\partial k} \right) K\left(\frac{1}{k^2}\right)
\end{aligned} \tag{27}$$

$$\begin{aligned}
G_7 &= \frac{\sqrt{2}}{\pi} \int_{-1}^{\infty} d\alpha (\langle \cos^2 \xi \rangle - \langle \cos \xi \rangle^2) \frac{\partial^2 g}{\partial \alpha^2} \\
&\quad \times \int_{-\pi}^{\pi} \frac{d\xi}{(\cos \xi + \alpha)^{1/2}} \\
&= \frac{4}{\pi} \int_1^{\infty} \frac{dk}{k} (\langle \cos^2 \xi \rangle_{out} - \langle \cos \xi \rangle_{out}^2) \\
&\quad \times \frac{\partial}{\partial k} \left( \frac{1}{4k} \frac{\partial g}{\partial k} \right) K\left(\frac{1}{k^2}\right)
\end{aligned} \tag{28}$$

Where,  $\lambda(\psi) = \frac{w}{\sqrt{2}} g(\alpha)$  and  $g(\alpha) = (\sqrt{\alpha} - 1)$  for outer region. All the integrals are contributed only in the outer regions because  $g(\alpha)$  is zero in the inner region. Here,

$$\langle \cos^2 \xi \rangle_{out} = -\frac{4}{3} \frac{E(\frac{1}{k^2})}{K(\frac{1}{k^2})} k^2 (2k^2 - 1) + \frac{8}{3} k^2 (k^2 - 1) + 1$$

For neoclassical term, we have calculated  $G_2$  as,

$$\begin{aligned}
G_2 &= -1.46 \sqrt{2} \pi \int_{-1}^{\infty} d\alpha \langle \cos \xi \rangle \frac{\Theta(\alpha - 1)}{\int_{-\pi}^{\pi} d\xi (\cos \xi + \alpha)^{1/2}} \\
&= -1.46 \pi \int_1^{\infty} \frac{dk}{E(\frac{1}{k^2})} \langle \cos \xi \rangle_{out}
\end{aligned} \tag{29}$$

Here the step function  $\Theta$  is taking care of the fact that the pressure gets flattened inside the island.

- [1] I. Hofman. Plasma Phys., **17**,143 (1975).
- [2] R.B. Paris and W. N-C. Sy. Phys. Fluids, **26**, 2966 (1983).
- [3] A. Bondeson and M. Persson. Phys. Fluids, **29**, 2997 (1986).
- [4] G. Einaudi and F. Rubini. Phys. Fluids, **29**, 2563 (1986).
- [5] X.L. Chen and P.J. Morrison. Phys. Fluids, B **2**, 495 (1990).
- [6] L. Ofman et.al. Phys. Fluids B, **3** 143 (1991).
- [7] K.P. Wessen and M. Persson. J. Plasma Phys., **4**, 267 (1991).
- [8] M. Persson and A. Bondeson. Phys. Fluids, B **2**, 2315 (1990).

- [9] X.L. Chen and P.J. Morrison. Phys. Fluids B, **4**, 845 (1992).
- [10] Ding Li and Chuanbing Wang. Phys. Plasmas, **2**, 1026 (1995).
- [11] R.L. Dewar and M. Persson. Phys. Fluids B, **5**, 4274 (1993).
- [12] M.S. Chu et.al. Phys. Plasmas, **2**, 2236 (1995).
- [13] D. Chandra, A. Sen, P. Kaw, M.P. Bora and S. Kruger, Nucl. Fusion **45**, 524 (2005).
- [14] R.J. Buttery, S. Gerhardt, A. Isayama *et al*, Procs. IAEA Fusion Energy Conference, Geneva, 2008, paperIT/P6-8.
- [15] ITER Physics Expert Group on Disruptions, Plasma Control and MHD, ITER Physics Basis Editors, Nucl. Fusion **39**, 2251 (1999).
- [16] R.J. LaHaye, 51st Annual Meeting of APS-DPP, Invited Talk GI3.00003
- [17] A.I. Smolyakov, Plasma Phys. Controlled Fusion **35**, 657 (1993).
- [18] A.I. Smolyakov, A. Hirose, E. Lazzaro, G.B. Re and J.D. Callen, Phys. Plasmas **2**, 1581 (1995).
- [19] H.R. Wilson et al, Phys. Plasmas **3**, 248 (1996).
- [20] F.L. Waelbroeck and R. Fitzpatrick, Phys. Rev. Lett., **78**, 1703 (1997).
- [21] J.W. Connor, F.L. Waelbroeck and H.R. Wilson, Phys. Plasmas **8**, 2835 (2001).
- [22] D. Chandra, A. Sen and P. Kaw, Nucl. Fusion **47**, 1238 (2007).
- [23] S.E. Kruger, C. Hegna and J. Callen, Phys. Plasmas, **5**, 4169 (1998).
- [24] R.B. White, D. Monticello, M.N. Rosenbluth and B.V. Wadell, Phys. Fluids **20**, 800 (1977).